Eur. Phys. J. B (2012) 85: 80
DOI: 10.1140/epjb/e2012-20953-1

THE EUROPEAN PHYSICAL JOURNAL B

Regular Article

Nature of optical properties of $GdFe_3(BO_3)_4$ and $GdFe_{2.1}Ga_{0.9}(BO_3)_4$ crystals and other $3d^5$ antiferromagnets

A.V. Malakhovskii[a], A.L. Sukhachev, A.D. Vasil'ev, A.A. Leont'ev, A.V. Kartashev, V.L. Temerov, and I.A. Gudim

L.V. Kirensky Institute of Physics, Siberian Branch, Russian Academy of Sciences, Akademgorodok, 660036 Krasnoyarsk, Russian Federation

Received 24 November 2011 / Received in final form 23 January 2012
Published online 27 February 2012 –

Abstract. Influence of the partial substitution of paramagnetic Fe^{3+} ions by diamagnetic Ga^{3+} ions in the trigonal crystal $GdFe_3(BO_3)_4$ on its optical and magnetic properties is studied and discussed in connection with problems common for all antiferromagnets containing $3d^5$ ions. Polarized optical absorption spectra and linear birefringence of $GdFe_3(BO_3)_4$ and $GdFe_{2.1}Ga_{0.9}(BO_3)_4$ single crystals have been measured in the temperature range 85–293 K. Specific heat temperature dependence (2–300 K) and structure of $GdFe_{2.1}Ga_{0.9}(BO_3)_4$ crystal have been also studied. As a result of substitution of 30% Fe to Ga the Neel temperature diminishes from 38 till 16 K, the strong absorption band edge shifts on 860 cm^{-1} (0.11 eV) to higher energy and the *d-d* transitions intensity decreases substantially larger than the Fe concentration does. Strong absorption band edge is shown to be due to Mott-Hubbard transitions. Correlation between position of the strong absorption band edge and the Neel temperature of antiferromagnets has been revealed. Properties of the doubly forbidden *d-d* transitions in the studied crystals and in other antiferromagnets are explained within the framework of the model of the exchange-vibronic pair absorption, which is theoretically analyzed in detail. The model permitted us to determine the connection between parameters of *d-d* absorption bands (intensity, width and their temperature dependences), on the one hand, and the exchange, spin-orbit and electron-lattice interactions, on the other hand.

1 Introduction

Crystals with the general formula $RM_3(BO_3)_4$ (R–Y or rare earth (RE) metal, M–Al, Ga, Cr, Fe, Sc) have huntite like structure with the trigonal space group *R32* (D_3^7) (No. 155 of the international tables for X-ray crystallography) [1]. Aluminates from this family possess good luminescent and nonlinear optical properties (see, e.g. Ref. [2]). RE ferroborates $RFe_3(BO_3)_4$ attract attention due to variety of magnetic structures and phase transitions realized in them depending on a choice of the RE ion and owing to interaction of two magnetic subsystems: Fe and RE elements [3]. Some of these crystals ($GdFe_3(BO_3)_4$, in particular) refer to multiferroics [4–8], which possess magnetic and electric order simultaneously. A coupling between static electric and magnetic subsystems observed in multiferroic materials is the effect interesting both for fundamental physics and potential technological applications [9–11]. Due to this property, ferroborates with the huntite structure are widely investigated in recent years.

Magnetic properties of $GdFe_3(BO_3)_4$ crystal were investigated in references [12–14]. Antiferromagnetic ordering phase transition takes place at 38 K. At $T < 9$ K, $GdFe_3(BO_3)_4$ crystal transforms from easy plane to easy axis antiferromagnet. Mössbauer spectra of $GdFe_3(BO_3)_4$ were measured in reference [15]. Magnetic properties of $GdFe_{2.1}Ga_{0.9}(BO_3)_4$ crystal were studied by Bezmaternykh et al. [16].

Crystal structure of $GdFe_3(BO_3)_4$ has been determind in reference [17]. The unit cell contains three formula units. Trivalent RE ions occupy only one type positions. They are located at the center of trigonal prisms made up of six crystallography equivalent oxygen ions. The FeO_6 octahedrons share edges in such a way that they form helicoidal chains, which run parallel to the C_3 axis and are mutually independent. In the $GdFe_3(BO_3)_4$ crystal at room temperature, all Fe ions occupy C_2-symmetry positions and Gd ions are in D_3-symmetry positions [17]. Such positions are the character of unperturbed huntite structure. The $GdFe_3(BO_3)_4$ crystal exhibits a structural phase transition to the symmetry $P3_121(D_3^4)$ [17] at 156 K [18]. At 90 K the local symmetry of Gd^{3+} ion is C_2 and Fe^{3+} ions are in two nonequivalent positions with C_2 and C_1 symmetries [17].

Optical absorption spectra corresponding to electron transitions inside $4f$ shell of RE ions (f-f transitions) were studied in the ferroborates in a number of works

[a] e-mail: malakha@iph.krasn.ru

(see, e.g., [19] and references therein). These spectra were mainly used as a tool for study of magnetic properties of the crystals. In $GdFe_3(BO_3)_4$, f-f transitions are in ultra violet and are not observed, since they are overlapped with the strong absorption band. Only transitions inside $3d$ shell of Fe^{3+} ions (d-d transitions) are observed in the spectrum. Optical absorption spectrum of $GdFe_3(BO_3)_4$ was first presented and discussed in references [20–22]. Transformation of the $GdFe_3(BO_3)_4$ absorption spectrum under the action of high pressure was studied in reference [20].

Absorption spectra of crystals under consideration consist of the strong absorption owing to allowed transitions and of the weak absorption bands corresponding to doubly forbidden (by parity and by spin selection rules) d-d transitions in the Fe^{3+} ions. Investigation of the strong absorption in the iron containing compounds goes back to works of Clogston [23] and Wickersheim and Lefever [24] and continues so far ([21,25–30] and references therein). In particular, in references [28,29] arguments were presented, that the allowed charge transfer transitions play an important role in the magnetoelectric coupling in strongly correlated $3d$ oxides. However, nature of the strong absorption band edge, whose position is substantially different in different Fe^{3+} compounds, remains to be under discussion.

Parity forbidden and doubly forbidden d-d transitions both in impurities and in antiferromagnets were studied in a great number of works (e.g., Refs. [31–35] and references therein). It was found that doubly forbidden d-d transitions are substantially more intensive in antiferromagnets than in impurity crystals. Tanabe et al. [36] suggested effective mechanism, which remove the spin-forbiddenness of the transitions due to pair absorption by the exchange coupled ions. It was widely used for analysis of the intensity of the doubly forbidden d-d transitions both in single pairs and in antiferromagnets (see e.g., [37–44]). However this mechanism could explain not all properties of the considered transitions, since it did not take into account the parity forbiddenness of the transitions. Malakhovskii and Vasiljev [45,46] proposed exchange-vibronic mechanism of the pair absorption, which provides simultaneous allowance of the transitions by spin and by parity selection rules. Some properties and consequences of this mechanism were presented in references [46–48]. However, a number of questions were still considered not in detail, e.g.: unusual temperature dependence of the doubly forbidden transitions intensity in antiferromagnets, degree of correlation between the intensity and the exchange interaction, role of the spin-orbit interaction in formation and probability of the exchange and exchange-vibronic absorption, role of the crystal phonons in the collective absorption. In this paper we comprehensively analyze properties of the exchange-vibronic absorption, basing on the conception of formation and relaxation of the exciton-magnon-phonon bound state, appeared as a result of a photon absorption by the pair of the exchange coupled ions. Obtained results are applied to interpretation of the doubly forbidden d-d transitions properties in $GdFe_3(BO_3)_4$ and $GdFe_{2.1}Ga_{0.9}(BO_3)_4$ crystals and in other antiferromagnetic compounds as well. Comparative study of $GdFe_3(BO_3)_4$ and the crystal with part of Fe^{3+} ions substituted by diamagnetic ions, substantially helps us to analyze the nature of absorption spectra of the magnetically ordering compounds.

Table 1. Atomic coordinates and equivalent displacement parameters for $GdFe_{2.1}Ga_{0.9}(BO_3)_4$ crystal at room temperature.

Atom	x	y	z	U_{eq}
Gd	0	0	0	0.0058(1)
Fe, Ga	0.21692(9)	1/3	1/3	0.0041(3)
O1	0.1449(4)	0.1449(4)	0.5	0.0052(6)
O2	0.4093(5)	0.4093(5)	0.5	0.0104(8)
O3	0.0264(4)	0.2135(4)	0.1835(4)	0.0075(4)
B1	0	0	0.5	0.002(1)
B2	0.5521(7)	0.5521(7)	0.5	0.0072(8)

Table 2. Distances Fe–O in crystals.

	Distances Fe–O (Å)	Ref.
$GdFe_{2.1}Ga_{0.9}(BO_3)_4$	2.028, 2.004, 1.945	This work
$GdFe_3(BO_3)_4$	2.032, 2.014, 1.96	[17]
$FeBO_3$	2.028	[50]

2 Results and discussion

Single crystals of $GdFe_3(BO_3)_4$ and $GdFe_{2.1}Ga_{0.9}(BO_3)_4$ were grown using the $K_2Mo_3O_{10}$-based flux as described in reference [12]. A small amount of neodymium oxide (Nd_2O_3/Gd_2O_3 = 0.9 mass% in the melt) was also introduced in $GdFe_{2.1}Ga_{0.9}(BO_3)_4$ crystal for future investigations of processes connected with magnetic transformations. The samples prepared for optical measurements were 0.1–0.3 mm-thick plane-parallel polished plates oriented perpendicular to the threefold crystallographic axis (C_3), and also cut in planes {100} and {110}, which are parallel to the C_3 axis.

We have undertaken the X-ray study of the $GdFe_{2.1}Ga_{0.9}(BO_3)_4$ crystal with the single crystal diffractometer KM-4 (MoK_α-radiation) at room temperature. A structure model was solved and refined in anisotropic approximation using SHELX-97 program [49]. It has been shown that the structure of the $GdFe_{2.1}Ga_{0.9}(BO_3)_4$ crystal is identical to that of $GdFe_3(BO_3)_4$. So, the crystal belongs to space group $R32$ and has the sell parameters $a = 9.499(1)$, $c = 7.521(1)$ Å, a little smaller than those of the $GdFe_3(BO_3)_4$ [17]. Atomic coordinates are shown in Table 1. Distance Gd–O in prisms is 2.361(3) Å. Fe–O distances in octahedrons are given in Table 2. The distortion of triangular prisms GdO_6 results from the rotation of triangular bases relatively to each other by 13 . Within the $(Fe/Ga)O_6$ chain the site of Fe^{3+} ion is filled randomly by Fe and Ga ions in proportion, corresponding to the chemical formula of the compound. It was found out, that the crystal consists of inversion twins in proportion of 59/41. Data shown in Table 1 refer to twins with the 59% contribution.

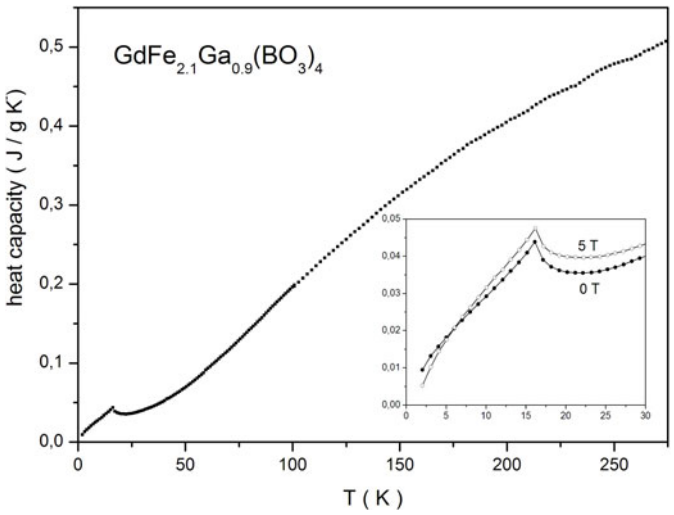

Fig. 1. Heat capacity of $GdFe_{2.1}Ga_{0.9}(BO_3)_4$ in zero magnetic field as a function of temperature. Insert: a part of the same dependence and in magnetic field of 5 T.

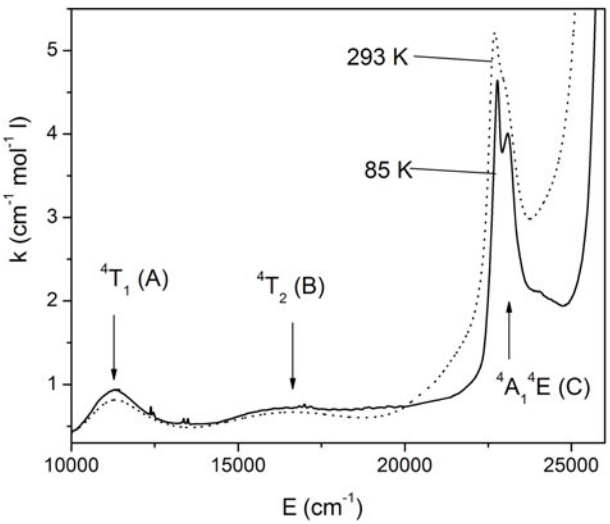

Fig. 2. $\sigma(\alpha)$ polarized absorption spectra of $GdFe_{2.1}Ga_{0.9}(BO_3)_4$.

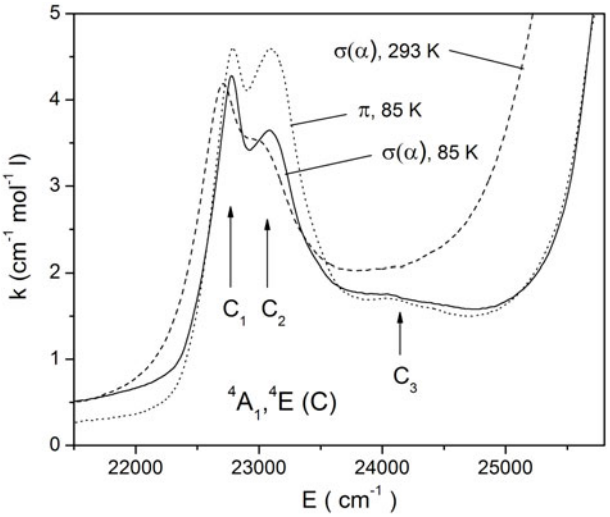

Fig. 3. Polarized absorption spectra of $GdFe_{2.1}Ga_{0.9}(BO_3)_4$ in the region of *d-d* transition $^6A_1(^6S) \rightarrow {}^4A_1{}^4E(^4G)$ of Fe^{3+} ion.

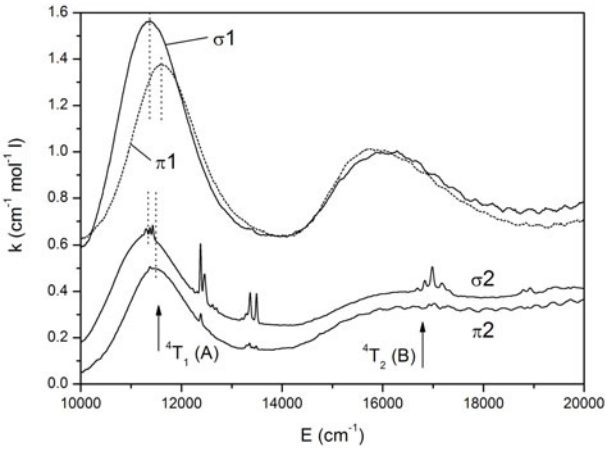

Fig. 4. Polarized absorption spectra of $GdFe_3(BO_3)_4(\pi 1, \sigma 1)$ and $GdFe_{2.1}Ga_{0.9}(BO_3)_4(\pi 2, \sigma 2)$ in the region of *d-d* transitions $^6A_1(^6S) \rightarrow {}^4T_1(^4G)$, $^4T_2(^4G)$ of Fe^{3+} ion at temperature $T = 85$ K.

Specific heat measurements of the $GdFe_{2.1}Ga_{0.9}(BO_3)_4$ crystal were performed by a commercial heat capacity measuring system (quantum design, PPMS) in the temperature range 2–300 K (Fig. 1). A feature at $T = 16$ K corresponds to a magnetic phase transition. According to magnetic measurements [16] it is the transition to the easy axis antiferromagnetic state, which remains at least down to 4.2 K. In the region of 3 K the Schottky-type anomaly in the heat capacity temperature dependence is observed (Fig. 1, insert) similar to that observed in $GdFe_3(BO_3)_4$ [51].

Polarized absorption spectra of $GdFe_{2.1}Ga_{0.9}(BO_3)_4$ and $GdFe_3(BO_3)_4$ crystals have been studied in the region of 390–1000 nm (10 000–25 600 cm^{S1}) and in the temperature range: 85–293 K. Three light polarizations were used: α – light wave vector $\vec{k}$ is parallel to C_3 axis of the crystal and, consequently, electric vector $\vec{E}$ of light is perpendicular to C_3 axis; $\pi - \vec{k} \perp C_3$, $\vec{E} \| C_3$; $\sigma - \vec{k} \perp C_3$, $\vec{E} \perp C_3$. Precise positions of polarization parallel or perpendicular to C_3 crystal axes were found according to minimum transparency of the sample in crossed polarizers. The measurements were carried out on the two-beam home made automatic spectrometer, based on the diffraction monochromator MDR-2. Optical slit-widths were 0.2−0.4 nm.

Figure 2 presents the total $\alpha(\sigma)$ absorption spectrum of $GdFe_{2.1}Ga_{0.9}(BO_3)_4$ crystal at two temperatures. In Figures 3–5, different parts of the $GdFe_{2.1}Ga_{0.9}(BO_3)_4$ and $GdFe_3(BO_3)_4$ spectra are given at different polarizations and temperatures. The absorption is given in units of the decimal molar extinction relative to molar concentration of iron that permits to take into account the difference of the iron concentration in the studied crystals. Molar concentration of iron is 25.02 mol/l in $GdFe_3(BO_3)_4$ and 17.51 mol/l in $GdFe_{2.1}Ga_{0.9}(BO_3)_4$. The observed broad absorption bands correspond to *d-d* transitions $^6A_1(^6S) \rightarrow {}^4T_1(^4G)$ (A-band), $\rightarrow {}^4T_2(^4G)$

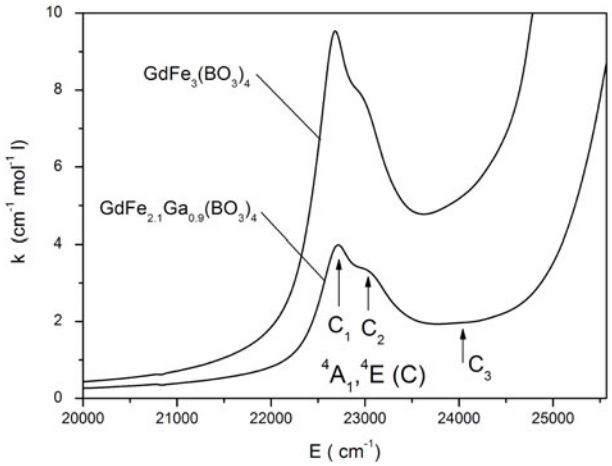

Fig. 5. α-polarized absorption spectra of $GdFe_3(BO_3)_4$ and $GdFe_{2.1}Ga_{0.9}(BO_3)_4$ in the region of *d-d* transition $^6A_1(^6S) \rightarrow {}^4A_1\,{}^4E(^4G)$ of Fe^{3+} ion at room temperature.

(B-band) and $\rightarrow {}^4A_1\,{}^4E(^4G)$ (C-band) in Fe^{3+} ($3d^5$) ion (in notations of cubic crystal field). Narrow lines in the $GdFe_{2.1}Ga_{0.9}(BO_3)_4$ spectra belong to *f-f* transitions in the small admixture of Nd^{3+} ions and will not be discussed. Gd^{3+} ions have no transitions in this spectral region. α and σ spectra practically coincide, that testifies to electric dipole character of the transitions. *d-d* absorption reveals some dichroism (Figs. 3 and 4) due to small trigonal distortions of FeO_6 octahedrons (Tab. 2). Presented spectra consist of two parts of the principally different nature: weak doubly forbidden (by parity and spin selection rules) *d-d* transitions and allowed transitions, forming the strong absorption band (only the edge of the band is observed). We shall consider these parts separately.

2.1 Strong transitions

Alumoborates $RAl_3(BO_3)_4$ are transparent till ~34 000 cm^{-1} (besides weak *f-f* transitions) independent of the rare earth ion. Strong absorption band edge of ferroborates $RFe_3(BO_3)_4$ is near 25 000 cm^{-1} (3.1 eV) and also almost independent of the rare earth ion. Thereby, the strong absorption in the visible is due to iron ions. There are three possibilities for the strong absorption connected with Fe^{3+} ions. (1) Allowed $d \rightarrow p$ transitions inside the Fe^{3+} ion with the energy ~10^5 cm^{-1}. (2) Allowed charge transfer transitions $2p \rightarrow 3d$ between molecular $2p$-orbitals of ligands and $3d$-orbitals of the Fe^{3+} ion inside FeO_6 cluster. In octahedral complex Fe^{3+}:Al_2O_3 the first of $2p \rightarrow 3d$ transitions occurs at 38 550 cm^{-1} (4.78 eV) [52]; in $Y_3Fe_5O_{12}$ and in $Y_3Ga_5O_{12}$:Fe^{3+} – at 35 600 cm^{-1} (4.41 eV) and 37 400 cm^{-1} (4.64 eV), respectively [53]; in $GdFe_3(BO_3)_4$ – at 4.0 and 4.8 eV, depending on polarization [21]. (3) Interatomic Fe−Fe *d-d* excitations (the Mott-Hubbard transitions):

$$3d^5 + 3d^5 + E_g \rightarrow 3d^4 + 3d^6. \quad (1)$$

These transitions occur between $3d$ states, i.e., they are forbidden in the first approximation by parity and also by spin selection rules, if total spins of the ions in the ground state have the same directions. However, the transitions are spin allowed if they take place between antiferromagnetically exchange coupled ions with the opposite spin orientations. Parity forbiddeness is removed, since the pair of atoms under consideration has no center of inversion at least in the excited state. Thus, these transitions can be considered as partially parity allowed ones without participation of odd vibrations. They are weaker than $2p \rightarrow 3d$ transitions between molecular orbitals of the cluster, but much stronger than *d-d* transitions inside $3d$ ions. The strong absorption band edge of the studied crystals is in the region of 25 000 cm^{-1} (3.1 eV), i.e. far from the mentioned $2p \rightarrow 3d$ transitions, whose position weakly depends on the Fe^{3+} concentration. Therefore we can suppose that the observed strong absorption band edge refers to the Mott-Hubbard transitions.

Pair states in the left and right sides of equation (1) give rise to the Mott-Hubbard bands. Activation energy (or insulating gap or optical gap [35,54]) is equal to:

$$E_g = U - (B_1 + B_2)/2. \quad (2)$$

Here $U = E(d^4 + d^6) - E(2d^5)$ is the electron correlation energy modified by the crystal field (CF) and covalency. In particular, instead of one transition between high spin states in the free ion approximation (1) we have four transitions in the cubic CF approximation:

$$^6A_1, {}^6A_1 \rightarrow {}^5E\left(d^4\right), {}^5T_2\left(d^6\right); {}^5T_2\left(d^4\right), {}^5T_2\left(d^6\right);$$
$$^5E\left(d^4\right), {}^5E\left(d^6\right); {}^5T_2\left(d^4\right), {}^5E\left(d^6\right). \quad (3)$$

The first of these transitions has the lowest energy. B_1 and B_2 in (2) are the lower and upper Mott-Hubbard band widths, respectively. The activation energy should also include the kinetic energy of the electron transfer. With the substitution of Fe by diamagnetic ions, the band widths B_1 and B_2 should, evidently, decrease and, consequently, the optical gap E_g should increase. Indeed, the strong absorption band edge in $GdFe_{2.1}Ga_{0.9}(BO_3)_4$, where part of Fe atoms is substituted by Ga atoms, is shifted to higher energy on ~860 cm^{-1} (0.11 eV) as compared with $GdFe_3(BO_3)_4$ (Fig. 5). This observation confirms the supposition that the strong absorption band edge refers to the Mott-Hubbard transitions. Transitions of such kind are connected not only with the change of state of an electron, but also with its space motion. Consequently, they are not vertical ones in the wave vector presentation. Therefore, according to the momentum conservation law, the transition can be possible only with the participation of phonons (indirect transitions), since momentum of photon is close to zero. (If these phonons are odd, they additionally allow the transition by parity.) The single particle band theory is not suitable for systems with the strong correlations such as the considered ones. Nevertheless, some its results can be used. It is known [55] that the coefficient of absorption for the allowed direct

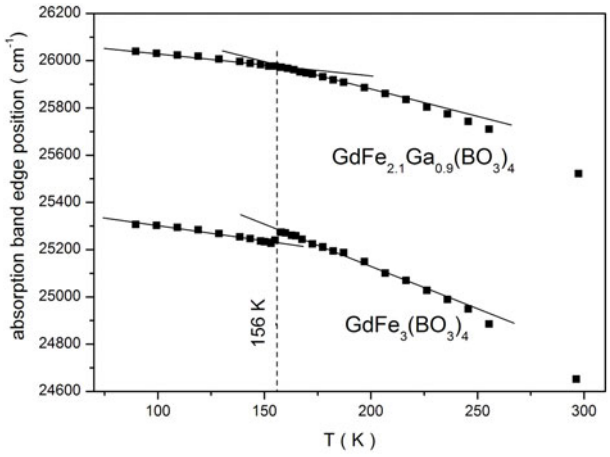

Fig. 6. Temperature dependence of the strong absorption band edge position on the level of $k = 8$ cm^{-1} mol^{-1} l in $GdFe_3(BO_3)_4$ and $GdFe_{2.1}Ga_{0.9}(BO_3)_4$ in σ-polarization.

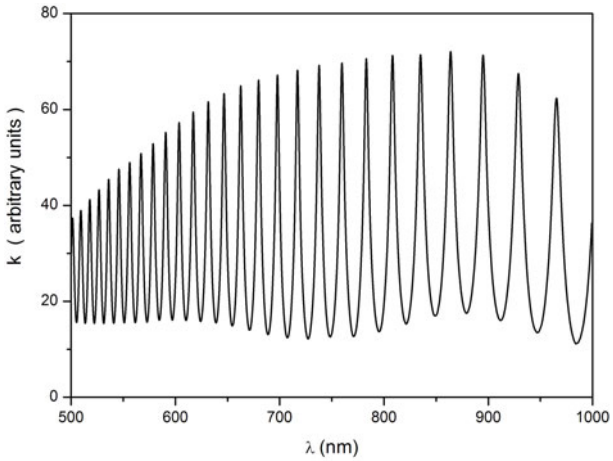

Fig. 7. Oscillations of the absorption coefficient of the system: sample of $GdFe_{2.1}Ga_{0.9}(BO_3)_4$ cut in {110} plane and positioned between two polarizers at room temperature (details are in the text).

transitions between parabolic bands is described by the formula:

$$k \sim (h\nu - E_g)^{1/2}. \tag{4}$$

The absorption coefficient for the indirect transitions is described by the parabolic function of the photon energy [55]:

$$k = \frac{A_1 (h\nu - E_g + E_p)^2}{\exp \frac{E_p}{k_B T} - 1} + \frac{A_2 (h\nu - E_g - E_p)^2}{1 - \exp\left(-\frac{E_p}{k_B T}\right)}. \tag{5}$$

Here E_p is the energy of the active phonon. The first term refers to absorption of the phonon and the second one refers to emission of the phonon. The experimental absorption band edge (Fig. 5) is indeed described well by a parabolic function and certainly is not described by the formula (4) in agreement with the indirect Fe−Fe transition nature of the band edge. Besides that, at constant E_g, the energy of the absorption band edge should decrease with the increasing temperature according to (5) – the very thing observed in the experiment (Fig. 6). The temperature behavior of the strong absorption band edge position (Fig. 6) should also reflect the variation of the insulating gap energy with the temperature. The temperature variation of the insulating gap is caused by the thermal lattice expansion and by the electron-phonon interaction variation [55]. It is evident that at structural phase transition both of these contributions change and should result in a singularity in the band gap temperature dependence. In particular, a pronounced shift of the absorption band edge was observed in $GdFe_3(BO_3)_4$ during structural phase transition under the influence of pressure [20]. At temperature 156 K of the $GdFe_3(BO_3)_4$ structural phase transition a jump of the $GdFe_3(BO_3)_4$ band edge position and a jump of its first temperature derivative are observed (Fig. 6). In the similar dependence for $GdFe_{2.1}Ga_{0.9}(BO_3)_4$ (Fig. 6) only a jump of the first derivative is observed at the same temperature. In the heat capacity temperature dependence of $GdFe_{2.1}Ga_{0.9}(BO_3)_4$ no singularities were observed (Fig. 1). The jump of the first derivative of the band edge temperature dependence at 156 K both in $GdFe_3(BO_3)_4$ and $GdFe_{2.1}Ga_{0.9}(BO_3)_4$ testifies to the similar features in the temperature behavior of the lattice parameters and of the electron-phonon interaction in these crystals, which, nevertheless, are not realized in a structural phase transition in the $GdFe_{2.1}Ga_{0.9}(BO_3)_4$ crystal.

Refractive index and birefringence in the region of weak absorption are mainly due to the strong absorption bands aside of this region. The birefringence of $GdFe_{2.1}Ga_{0.9}(BO_3)_4$ and $GdFe_3(BO_3)_4$ crystals has been measured in {110} plane in the following way. We put the sample between two polarizers with the same plane of polarization so that C_3 axis of the sample was under the angle of 45 to the plane of polarization. In this case, due to interference of the usual and unusual waves after the analyzer, the light flow passed through the analyzer oscillates as a function of the light wave length. An example of such oscillations for $GdFe_{2.1}Ga_{0.9}(BO_3)_4$ is depicted in Figure 7. Phase difference between two normal waves is

$$\varphi = 2\pi \Delta n d/\lambda, \tag{6}$$

where Δn is the birefringence, λ is the wave length and d is the width of the sample. A change of the phase difference ($\Delta\varphi$) corresponding to the distance $\Delta\lambda$ between two adjacent maxima or minima of the periodical structure of Figure 7 should be equal to 2π, and according to (6)

$$|\Delta\varphi| = 2\pi \Delta n d \Delta\lambda/\lambda^2 = 2\pi \tag{7}$$

under the assumption that $\Delta\lambda \ll \lambda$. Then

$$\Delta n = \lambda^2/d\Delta\lambda. \tag{8}$$

Results of calculations are in Figure 8 (temperature influences the birefringence very weakly). It is seen, that, indeed, only the most intensive d-d transition (C-band)

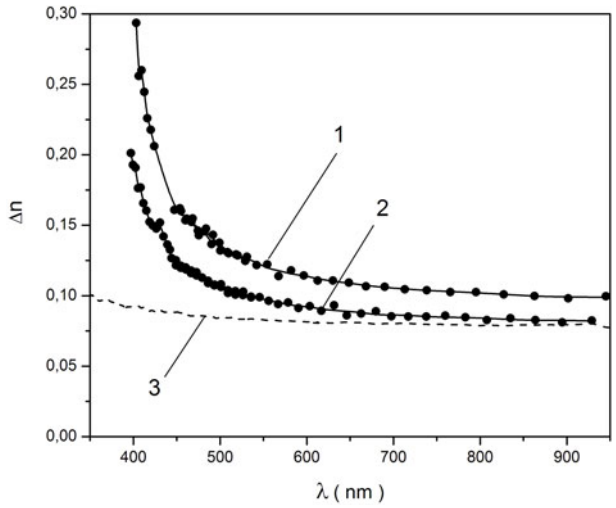

Fig. 8. Birefringence of $GdFe_3(BO_3)_4$ (curve 1), $GdFe_{2.1}Ga_{0.9}(BO_3)_4$ (curve 2) and $Y_{0.6}Yb_{0.3}Tm_{0.1}Al_3(BO_3)_4$ (curve 3) in the plane {110} at room temperature.

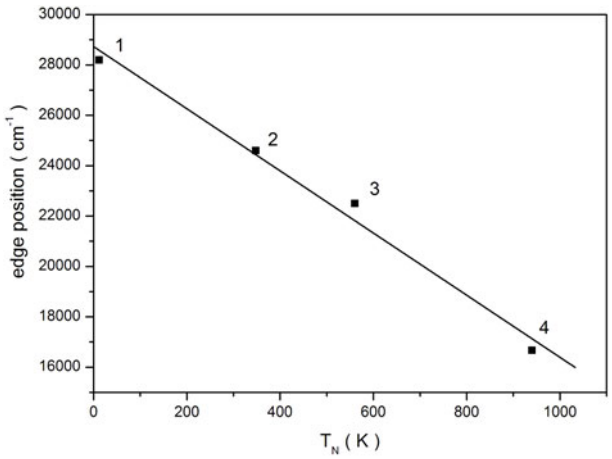

Fig. 9. Correlation between position of the strong absorption band edge and temperature of the magnetic ordering. 1 – $Ca_3Fe_2Ge_3O_{12}$ (Ref. [56]), 2 – $FeBO_3$ (Ref. [57]), 3 – $Y_3Fe_5O_{12}$ (Ref. [58]), 4 – $Li_{0.5}Fe_{2.5}O_4$ (Ref. [59]).

slightly influences the birefringence. Similar measurements of the birefringence were carried out on ferroborates $RFe_3(BO_3)_4$ with different RE ions. Results weakly depend on RE ions, but substantially differ from those for alumoborates of the same structure (see Fig. 8). In the ferroborates the birefringence strongly increases near the absorption band edge. Consequently, contribution of transitions with participation of Fe^{3+} ions, and, especially, of the Fe−Fe (the Mott-Hubbard) transitions, into the birefringence is substantial. The birefringence value decreases with the decrease of the Fe concentration (Fig. 8) but less than strictly proportionally to the Fe concentration. It is due to additional contribution into the birefringence of transitions not connected with the Fe^{3+} ions.

The Fe−Fe (the Mott-Hubbard) transitions are conditioned by overlapping of the Fe^{3+} wave functions, modified by hybridization with wave functions of the environment. The same overlapping is the cause of the exchange interaction and magnetic ordering. Consequently, position of the strong absorption band edge in Fe^{3+} containing compounds should correlate with the temperature of their magnetic ordering. Figure 9 demonstrates such correlation. $GdFe_3(BO_3)_4$ and $GdFe_{2.1}Ga_{0.9}(BO_3)_4$ crystals can not be put in this row, since they are almost one dimensional magnetics, while all compounds used in Figure 9 are three dimensional ones. However, for the former two compounds the same correlation between their Neel temperatures and positions of the strong absorption band edge is also observed.

2.2 d-d transitions

Absorption spectra of the *d-d* transitions (Figs. 2–5) have been decomposed on Gauss components and integral intensities of the bands have been found. Results are shown in Table 3. It is seen, that intensities of the transitions are substantially larger in $GdFe_3(BO_3)_4$, than in $GdFe_{2.1}Ga_{0.9}(BO_3)_4$. Shape of the $GdFe_3(BO_3)_4$ absorption spectrum is qualitatively similar to that of the $FeBO_3$ spectrum [21], but intensity of the absorption bands in the former crystal is by order of magnitude less. Question arises: what is the cause of the observed differences of the transition intensities? Fe−O distances in all mentioned crystals are close in value (Tab. 2). As a consequence, parameters of the Fe-ligand interaction are similar. In particular, position of the A-band, which characterizes the cubic CF value for $3d^5$ ions, is almost the same in all three crystals (Fig. 4 and [21]). Intensity of *d-d* transitions strongly depends on covalency of the metal-ligand bonding [60], but position of the C-band, which characterizes degree of the covalency for $3d^5$ ions [60], is also practically identical in the discussed crystals (Fig. 5 and [21]). This means, that the covalency and the CF in these crystals are the same and are not the cause of the difference of the *d-d* transition intensities. Additionally, $FeBO_3$ is the centrosymmetrical crystal unlike $GdFe_3(BO_3)_4$ and $GdFe_{2.1}Ga_{0.9}(BO_3)_4$. Consequently, from the viewpoint of the transition allowance by parity, intensity of *d-d* transitions in $FeBO_3$ should be less than in $GdFe_3(BO_3)_4$ and $GdFe_{2.1}Ga_{0.9}(BO_3)_4$. All these inconsistencies should be solved.

Table 3. Oscillator strengths ($f \times 10^7$) of *d-d* transitions in $\sigma(\alpha)$ polarization.

Bands	$GdFe_3(BO_3)_4$		$GdFe_{2,1}Ga_{0,9}(BO_3)_4$	
	85 K	293 K	85 K	293 K
A	9.5	6.9	4.75	3.9
B	11.6	7.8	8.6	6.9
$C_1 + C_2$	21.6	23.3	7.3	9.5

Shape of the observed absorption spectra is typical for *d-d* transitions in $3d^5$ ions in centrosymmetrical crystals (for Mn^{2+} see e.g., Ref. [60]). This shape is the result of the electron-vibrational interaction with the quasi local odd

vibrations, which makes the transitions parity allowed. In particular, C_1, C_2 and C_3 components (Fig. 3) correspond to different vibrations, but to the same electronic transition (compare with Ref. [48]). The same vibrations take part in formation of the A- and B-bands as well, but the corresponding vibronic components are much wider and they overlap each other. Therefore, A- and B-bands are not strictly symmetric and usually require more than one Gauss curves for their description. The studied crystals have no center of inversion. However, narrow pure electronic transitions allowed by static non-centrosymmetrical components of the CF are too weak to be observed even at low temperature [21]. Thus, odd vibrations are more effective than the static odd distortions for allowance of the observed transitions by parity, though, from the symmetry point of view, they are equivalent.

We deal with the spin and parity forbidden *d-d* transitions. The spin forbiddenness in one ion approximation is shifted by the spin-orbit interaction, which is substantially quenched in 3*d* complexes by the strong CF. Effectiveness of this mechanism does not depend on the Fe^{3+} ions concentration. However, it was found (Tab. 3), that oscillator strengths of the transitions are larger in $GdFe_3(BO_3)_4$ as compared with that in $GdFe_{2.1}Ga_{0.9}(BO_3)_4$, especially as concerns the C-band. Thus, intensity of the transitions increases faster than the Fe^{3+} ion concentration does. This means that considered *d-d* transitions are due to the pair absorption by pairs of Fe^{3+} ions. As mentioned above, Tanabe et al. [36] suggested effective mechanism, which removes the spin-forbiddenness of a transition due to the pair absorption by exchange coupled ions. Vibrations, both odd and even, were widely used for interpretation of the fine structure of the doubly forbidden *d-d* transitions, but not as a source of the allowance by parity. However, in order to remove both parity and spin forbiddenness, it is necessary to take into account simultaneously electron-vibrational (vibronic) interaction of the orbitally excited ion with odd vibrations (V) and exchange interaction between ions of the pair (H^e) in Hamiltonian of the pair:

$$H = H_0 + H^e + V, \tag{9}$$

here H_0 is the unperturbed Hamiltonian of the pair. In the general case, the static odd distortions can be taken into account in the perturbation V as well, but in octahedral complexes odd vibrations are usually more effective even when the static odd distortions exist (as in our case, in particular). Spin-orbit interaction is not taken into account, since, according experiments, the exchange mechanism, when it exists, removes the spin-forbiddenness much more effectively than the spin-orbit mechanism does. In the first approximation of the perturbation theory the Hamiltonian (9) does not remove the double forbiddenness. In the second approximation of the perturbation theory, matrix element of the electric dipole moment of the doubly forbidden transition $i \to f$ is written in the form

$$D_{if}^{ev} = \sum_m D_{im} \sum_k \frac{H_{mk}^e V_{kf}}{E_{km} E_{fk}}. \tag{10}$$

Suppose that denominators in (10) are equal at all m and k. Then, using the formula for calculation of matrix elements of the product of operators, we obtain from (10)

$$D_{if}^{ev} = \frac{1}{E^2} \left(DH^e V\right)_{if}. \tag{11}$$

This equation is of course approximate. It will be exact provided the only one term in the sum (10) remains, but from the symmetry point of view it is strict.

Since the spin-orbit interaction was neglected in (9), the wave functions of the system can be written in the form: $\psi = \psi(r) \cdot \varphi(s)$, where $\psi(r)$ is the function of electron coordinates and $\varphi(s)$ is the function of the electron spins. Then from (11) we obtain the electric dipole matrix element of the doubly forbidden electron transition allowed by the exchange-vibronic mechanism

$$D_{if}^{ev} = \frac{1}{E^2} \left\langle \psi_f(r) \left| DV \right| \psi_i(r) \right\rangle \left\langle \varphi_f(s) \left| H^e \right| \varphi_i(s) \right\rangle, \tag{12}$$

i.e., variables are separated and probability of the doubly forbidden transition (W_{ev0}) is the product of probabilities of the vibronic (W_{v0}) and exchange (W_{e0}) absorption processes for the transitions forbidden only by parity or by spin selection rules respectively:

$$W_{ev0} = k_{ev} W_{v0} W_{e0}. \tag{13}$$

Coefficient k_{ev} contains in reality not only parameter E. It is a parameter of bonding (see below) between mentioned processes assumed to be independent in a first approximation. If the exchange interaction is written in the form: $H^e = J(\hat{s}_a \cdot \hat{s}_b)$, where $\hat{s}_a$ and $\hat{s}_b$ are spin operators of a and b ions, then for the pair absorption we have from (11) in the operator form

$$D^{ev} = \frac{1}{E^2} J(DV) \left(\hat{s}_a \cdot \hat{s}_b\right). \tag{14}$$

If instead of the vibronic Hamiltonian one takes some other interaction H_1, which removes the parity forbiddenness, then we shall obtain, as a particular case, the effective operator of the transition electric dipole moment for the exchange mechanism of the pair absorption:

$$D^e = \frac{1}{E^2} J\left(DH_1\right) \left(\hat{s}_a \cdot \hat{s}_b\right). \tag{15}$$

Interaction H_1 can be a consequence of lack of the static center of symmetry for the single ion or for the pair of the ions at least in the electronically excited state. As mentioned above, the static mechanism is less effective than the vibronic one for the allowance of *d-d* transitions by parity. If we introduce identification

$$\pi_{ab} = J\left(DH_1\right)/E^2, \tag{16}$$

we shall obtain from (15) the effective operator of the dipole moment, which exactly coincides with that introduced by Tanabe et al. [36]. Selection rules for matrix elements of the spin operator $(\hat{s}_a \cdot \hat{s}_b)$ in (14) and (15) ensure the breakdown of the spin forbiddenness of the transition

in one ion, when the pair absorption of light takes place: $\Delta s_a = 0, \pm 1$; $\Delta s_b = 0, \pm 1$; $\Delta s = 0$; $\Delta m_s = 0$, where s – is the total spin of the pair.

It is well known, that probability of the vibronic absorption of the only parity forbidden transition depends on temperature in the following way:

$$W_{v0} = W_\nu(0) \coth(\Omega/2kT). \tag{17}$$

All theoretical models for the intensity of the purely exchange ("exciton-magnon") absorption give $W_{e0} = \text{const.}(T)$ at $T > T_N$, if only thermal population of the magnetic states is taken into account [39–41]. Then intensity of the exchange-vibronic absorption W_{ev0} at $T > T_N$ should follow the function (17), i.e. it should increase approximately proportionally to the temperature. However it is not so: the absorption line intensities either slowly increase or slowly decrease (see Tab. 3 and, e.g., Ref. [45], concerning another $3d^5$ antiferromagnetic compounds). Consequently, some phenomena were not taken into account.

When a photon is absorbed by an atom of a periodic lattice, the electronic, vibrational or spin excitations can travel through the crystal as quasi particles: exciton, phonon or magnon. Depending on the coupling between them, the quasi particles can exist either in a free or in a bound state. If the quasi particles are free, highly mobile, and strongly delocalized, their interaction per photon-absorbing cluster is almost zero and the probability of the many-particle absorption is likewise very low. (By definition, completely free quasi particles do not interact.) However, the exciton, magnon and phonon can form a bound localized slow-moving excitation, which does not differ basically from the corresponding excitation of an impurity [61–63]. Additionally, the electronically excited atom is actually an impurity, since its electronic state differs from that of the surrounding atoms. The probability of the transition into the superposed configuration (in which all considered excitations are on the same site) is described in the first approximation by the local (cluster) models of the transition allowance presented above. Thus, if so-called "exciton-magnon" or "exciton-magnon-phonon" absorption is observed in a periodic crystal, this means that a fairly stable bound exciton-magnon or exciton-magnon-phonon state is created, when a photon is absorbed. However, even the stable bound state inevitably relaxes and disintegrates into free quasi particles. Lifetime of the bound state can influence the probability of the considered transition. If this lifetime (t) is larger than a time (t_0) of interaction of the photon with the pair of atoms (time of the photo-transition), than the probability of the transition W_0 is defined only by the operator (14) or (15), i.e., excited state can be considered as a quasi-stable one. If $t < t_0$, then the probability of the transition is $W = W_0 t/t_0$.

Let's assume that distribution of individual lifetimes of the bound excited state of the pair has the form: $\exp(-t/\tau)$ [64], where τ is the average lifetime. Then the probability of the pair transition is:

$$\begin{aligned} W &= W_0 \left(\int_{t_0} \exp\left(\frac{-t}{\tau}\right) dt \right. \\ &\quad \left. + \int_0^{t_o} \frac{t}{t_0} \exp\left(\frac{-t}{\tau}\right) dt \right) \Bigg/ \int_0 \exp\left(\frac{-t}{\tau}\right) dt \\ &= W_0 \frac{\tau}{t_0} \left(1 - \exp\left(\frac{-t_0}{\tau}\right)\right). \end{aligned} \tag{18}$$

The limit cases follow from (18):

$$W \approx W_0 = \text{const.}(\tau), \quad \text{when} \quad \tau \gg t_0, \tag{19}$$

$$W \approx W_0 \tau/t_0 \quad \text{when} \quad \tau \ll t_0. \tag{20}$$

The limit case (19) corresponds to the long living (quasi-stable) bound states. We shall consider the second limit case.

Probability of the excited state relaxation in the two level approximation is

$$W = A + B\rho(\varepsilon, T), \tag{21}$$

here A and B are the Einstein coefficients for the spontaneous and stimulated radiation, respectively, ε is the energy of the excited state and $\rho(\varepsilon, T)$ is the spectral density of radiation, which interacts with the excited pair of atoms, and it is equal to

$$\rho(\varepsilon, T) = \varepsilon f(\varepsilon)\, n(\varepsilon, T), \tag{22}$$

here $f(\varepsilon)$ is the spectral density of states of the field, interacting with the pair, $n(\varepsilon, T)$ are average occupation numbers of these states. If the system is in the thermal equilibrium with the radiation (with lattice phonons, in particular), then from the Boltzmann level population distribution: $N \sim \exp(-\varepsilon/kT)$ it follows [65]:

$$\frac{A}{B} = \rho(\varepsilon, T) \left[\exp\left(\frac{\varepsilon}{kT}\right) - 1\right]. \tag{23}$$

In the Bose-Einstein statistics: $n(\varepsilon, T) = [\exp(\varepsilon/kT) - 1]^{\check{S}\,1}$. Then from (23) and (22): $A/B = \varepsilon f(\varepsilon)$ and from (21):

$$\tau = 1/W = [1 - \exp(-\varepsilon/kT)]/B\varepsilon f(\varepsilon). \tag{24}$$

After substitution of (24) into (20) we find

$$W = \frac{W_0}{R} \left[1 - \exp\left(-\frac{\varepsilon}{kT}\right)\right]. \tag{25}$$

The parameter

$$R = t_0 B \varepsilon f(\varepsilon) \tag{26}$$

characterizes interaction of the pair (during time t_0 of the electron transition) with the environment, which leads to relaxation (disintegration) of the bound excited state.

Relaxations of the electronic, spin and vibrational excitations, which form the bound excited state, can be considered independent in a first approximation, but the relaxation of any of them means the relaxation of the whole bound state. Thus, the relaxation rate of the bound state approximately equals to the sum of the relaxation rates of all excitations, forming the bound state. The relaxation rate of the purely electronic excitation, corresponding to the doubly forbidden transition, is comparatively small and can be neglected. Then, according to (13), (17) and (25), the probability of the exchange-vibronic pair absorption ("exciton-magnon-phonon" absorption) is written in the form:

$$W_{ev} = k_{ev} W_{e0} W_\nu (0) \left[\frac{R(J)}{1 - \exp(-J/kT)} + \frac{R(\Omega)}{1 - \exp(-\Omega/kT)} \right]^{š\,1} \coth(\Omega/2kT). \quad (27)$$

Here W_{e0} – is the probability of the exchange absorption, introduced in (12) and (13). According to (14), $W_{e0} \sim J^2$. Values J and Ω – are energies of the local magnetic and odd vibrational excitations, respectively, $R(J)$ and $R(\Omega)$ – are parameters of relaxation, characterizing the interaction of the respective excitations with the lattice phonons. For the exchange pair absorption ("exciton-magnon" absorption) we have:

$$W_e = \frac{k_e W_{e0}}{R(J)} \left(1 - \exp \frac{-J}{kT}\right). \quad (28)$$

From the above consideration it is clear that expressions "exciton-magnon" and "exciton-magnon-phonon" absorption are actually traditional conventional expressions, especially when we deal with temperatures $T > T_N$. At temperatures $T > T_N$, as mentioned above, $W_{e0} = \text{const.}(T)$, and it describes the exchange absorption probability, when only thermal population of states is taken into account [39–41]. The same theories at $T < T_N$ give different functions for $W_{e0}(T)$, depending whether the long range or short range order model of the exchange coupling and absorption is accepted. In the former model, the ion states are split in the effective exchange field of the environment according to the spin projection M_S onto the direction of magnetic ordering. The electron transition becomes allowed with respect to the spin projection of the ion pair, because the spin projection of the ion located near the electronically excited ion changes in opposite direction. In the short-range order model, the exchange interaction of the ion pair is taken into account exactly and the effect of the rest of the crystal is included by introducing an effective field, which not only splits the states of the pair according to the projection of its total spin but also mixes the states that have different total spins $S(\Delta S = 1)$ and identical projections M_S [39]. In the long-range order model, as the temperature increases from 0 K to T_N, the intensity of the cold "exciton-magnon" absorption, strongly decreases [40], whereas in the short-range order model its intensity increases [41]. Thus, the predictions of these two models are substantially different. Analysis of experimental results at $T < T_N$ has shown [48], that in this temperature interval the long-range order model describes temperature behavior of the factor W_{e0} in the "exiton-magnon" lines intensity (28), while the short range order model is suitable for description of the same exchange factor in the exchange-vibronic absorption probability ("exiton-magnon-phonon" line intensity) in the formula (27). Vibronic factor (17) is almost constant in the region $T < T_N$.

Assuming $W_{e0} = \text{const.}(T)$ in all temperature range, we obtain from (27) at $T = 0$ K:

$$W_{ev} = k_{ev} W_{e0} W_\nu(0) \left[R(J) + R(\Omega)\right]^{š\,1}, \quad (29)$$

and at $T \to \infty$:

$$W_{ev} = k_{ev} W_{e0} W_\nu(0) \left[\frac{\Omega}{2J} R(J) + \frac{1}{2} R(\Omega)\right]^{š\,1}. \quad (30)$$

From (29) and (30) it is seen that, depending on correlation between parameters of relaxation of the local magnetic and odd vibrational excitations, probability of the exchange-vibronic absorption can be a weakly increasing or weakly decreasing function of temperature at $T > T_N$. This is the characteristic feature of the exchange-vibronic pair absorption, which distinguishes it from the purely vibronic absorption, whose intensity increases with the temperature rising without limit proportionally to $\coth(\Omega/2kT)$, and distinguishes it from the purely exchange pair absorption, whose intensity decreases quickly with the temperature rising both according to equation (28) and according to experiments [47] (see below). Intensities of the *d-d* transitions in $GdFe_3(BO_3)_4$ and $GdFe_{2.1}Ga_{0.9}(BO_3)_4$ change slowly and in different directions (see Tab. 3). Thus, they are due to exchange-vibronic pair absorption.

Competition of the spin-phonon and the local vibration-phonon relaxation processes is substantially influenced by the correlation between energies of the spin and vibrational excitations, on the one hand, and the energy of the lattice phonons, on the other hand. The energy of the spin excitations practically always lies in the energy band of the lattice phonons. Therefore these excitations have nice conditions both for the direct and Raman relaxation. Another situation takes place for the local vibrational excitations. In the electronically excited state, frequencies of the cluster vibrations, found from optical absorption spectra, appreciably differ from the crystal vibrations found from infra red spectra (see, e.g., Ref. [48]). These quasi local vibrations can leave the energy band of the corresponding optical lattice phonons, what results in the strong decrease of the local vibration relaxation rate.

Now we shall analyze the dependence of the probability of the exchange and exchange-vibronic absorption on the exchange interaction. According to (13) and (14):

$$W_{ev0} \sim W_{e0} \sim J^2. \quad (31)$$

If the local vibration-phonon relaxation rate prevails, then, according to (29) and (30), both in the low temperature and high temperature limits $W_{ev} \sim J^2$.

Table 4. Oscillator strengths ($f \times 10^7$) of *d-d* transitions in some compounds of Mn^{2+} and their changes at the temperature change between 77 and 300 K [68].

Crystal	T_N (K)	T (K)	f_A	Δf_A (%)	f_B	Δf_B (%)	f_C	Δf_C (%)
$MnCl_2{\cdot}4H_2O$	1.62	77	1.26		0.39		0.36	
		300	1.89	+50	0.55	+41	0.62	+72
$MnCl_2$	1.96	77	10.5		12.6		4.8	
		300	12.7	+21	12.2	−3.2	7.3	+52
$MnCl_2{\cdot}2H_2O$	6.8	77	4.01		2.59		1.56	
		300	3.48	−13	1.35	−48	2.65	+70
$MnCO_3$	29.5	77	2.92		3.20		8.34	
		300	3.16	+8	2.22	−30	7.70	−7.7

Suppose that the spin-lattice relaxation rate prevails. In the Debye approximation, the phonon density of states

$$f(\varepsilon) \sim \varepsilon^2. \tag{32}$$

Basing on references [66,67], devoted to the spin-phonon relaxation of the exchange subsystem (unlike the Zeeman subsystem in paramagnetic resonance), it is possible to write (26) in the Debye approximation:

$$R(J) = J^3 \left(\frac{\partial J}{\partial Q}\right)^2 \left(C_1 \frac{D^2}{J^2} + C_2 \frac{\lambda^2}{\Delta E^2}\right). \tag{33}$$

The components in (33) characterize contributions of modulation of the isotropic and anti symmetric exchange, respectively, by phonons into the spin-lattice relaxation rate. D is the constant of the dipole interaction, λ is the constant of S-L interaction in the excited state, ΔE is the distance between electron levels mixed by the S-L interaction, Q is the normal coordinate of the phonon active in the spin-lattice relaxation, C_1 and C_2 are scale coefficients, J is the constant of the exchange between electronically excited and not excited atoms, which is usually of the same order of magnitude as that in the ground state. If structures of the compared crystals are similar, then it is possible to consider that $\partial J/\partial Q \sim J$. Temperature range $T > T_N$ can be considered as the high temperature approximation for the exchange-vibronic absorption. Then from (33), (31) and (30) in the case of the isotropic exchange modulation we obtain $W_{ev} \sim W_e = \text{const.}(J)$, and in the case of the anti symmetric exchange modulation: $W_{ev} \sim W_e \sim J^{\check{S}\,2}$. At $T = 0$ (if not to take into account temperature dependence of W_{e0} in this region) we obtain, respectively, $W_{ev} \sim W_e \sim J^{\check{S}\,1}$ and $W_{ev} \sim W_e \sim J^{\check{S}\,3}$. The increase of the exchange and exchange-vibronic transitions intensity with the decreasing exchange constant seems to be paradoxical ex facte. However, when J decreases and, correspondingly, the relaxation time τ increases (see Eq. (24)), we shall come eventually to the situation $\tau \ll t_0$, when $W = W_0 \sim J^2$ according to (19) and (31). Secondly, we did not take into account yet properties of the coefficient of bonding between excitations, which forms the exciton-magnon or exciton-magnon-phonon bound state.

It is obvious, that the bond between mentioned two or three excitations of interest depends simultaneously on the exchange and S-L interaction or, roughly speaking, on the product of their parameters. When any of these parameters decreases, the bond can break down and the cooperative absorption will not take place. It is possible to identify the exchange-vibronic absorption by weak increasing or decreasing temperature dependence of its intensity at $T > T_N$. Having this in mind, let's analyze data of Table 4, where crystals are arranged in the order of the Neel temperature increase. It is seen that in $MnCl_2{\cdot}4H_2O$ all transitions are of the one-ion nature, in $MnCl_2$ and $MnCl_2{\cdot}2H_2O$ only the C-band is certainly conditioned by the one-ion absorption and in $MnCO_3$ all bands are due to the cooperative exchange-vibronic absorption. The difference in the behavior of the different bands can be accounted for by the role of the S-L interaction in the bonding of the excitations. Indeed, A- and B-bands are the transitions $A_1 \rightarrow T_1$ and $A_1 \rightarrow T_2$ to the states possessed the orbital moment and, consequently, possessed the S-L interaction, but the C-band is the transition $A_1 \rightarrow A_1E$ to the states not possessed the orbital moment and (in a first approximation) the S-L interaction (everything in the cubic CF). Therefore, as a result of the latter transition, the bound state is generated at the larger exchange interaction. Thus, the probability of the exchange-vibronic pair absorption is a complicated function of the exchange interaction. Nevertheless, it is in general an increasing function of the exchange interaction. Indeed, intensity of the *d-d* absorption bands in $GdFe_3(BO_3)_4$ ($T_N = 38$ K) is on the order of magnitude less than in $FeBO_3$ ($T_N = 348$ K) [21]. Intensity of A and ($C_1 + C_2$) bands (per ion) in $GdFe_{2.1}Ga_{0.9}(BO_3)_4$ ($T_N = 16$ K) is substantially smaller than in $GdFe_3(BO_3)_4$ (Tab. 3) since in the former case besides the pair absorption there is also the one-ion absorption of weak intensity (it is also possible to consider this fact as a correlation with T_N).

Intensity of the C-band is substantially larger than intensities of A- and B-bands (see Tab. 3). Sometimes this is referred to the borrowing of intensity from the close strong transitions. Such mechanism can take place in principle, but the same situation is typical also for antiferromagnetic $Mn^{2+}(3d^5)$ compounds, where there are no strong transitions close to the C-band (see $MnCO_3$ in Tab. 4 and also Ref. [60]). When the exchange-vibronic absorption is not observed, discussed bands are of the similar intensities or even they may be in opposite proportion (Tab. 4). Indeed, in the case of one ion absorption, the spin forbiddenness is

removed by S-L interaction. But, as it was noticed above, in the excited states A_1, E (C-band) S-L interaction in a first approximation is equal to zero, contrary to T_1 and T_2 states (A- and B-bands). In the pair absorption the spin forbiddenness is removed by the exchange interaction. S-L interaction enlarges the relaxation rate of the bound state and so, according to the above consideration, it diminishes the pair absorption probability. Thus, S-L interaction plays mainly the opposite role in formation of the intensity of the one ion and pair absorption.

In the $FeBO_3$ crystal ($T_N = 348$ K) at least up to 150 K a fine structure due to so called "exciton-magnon" transitions is observed on the transition $^6A_{1g} \rightarrow {}^4T_{1g}(^4G)$ (A-band) [69]. In $GdFe_3(BO_3)_4$ ($T_N = 38$ K) such structure on the same band is not observed even at 9 K [21]. On the transition $^6A_{1g} \rightarrow {}^4T_{2g}(^4G)$ (B-band) the fine structure is not observed in all enumerated above and in many other $3d^5$ compounds. At the same time, in $MnCO_3$ ($T_N = 32$ K) the similar structure on the transitions $^6A_{1g} \rightarrow {}^4T_{2g}(^4D)$ and $^6A_{1g} \rightarrow {}^4T_{1g}(^4P)$ is observed at temperatures much above T_N, but intensities of the narrow lines strongly decrease with the temperature rising contrary to behavior of the wide bands, corresponding to the "exciton-magnon-phonon" absorption [47]. All these properties can be qualitatively accounted for by the model described above. First of all, existence of the so called "exciton-magnon" lines at temperatures much higher T_N confirms, that we deal with the bound exciton-magnon states, which, more strictly, can be called and considered as electron-spin quasi local excitations. The observed "exciton-magnon" lines are allowed by parity without participation of odd vibrations. Indeed, it is well known that at temperature near 0 K the distance between the first "exciton-magnon" line and the purely electron (exciton) line is close to the energy of the spin excitation (magnon). Such absorption is partially parity allowed, since the pair absorbing a photon has no center of inversion at least in the excited state. Repetitions of the first line are due to even local vibrational excitations. Probability of the exchange pair absorption is described by the formula (28). First of all, we obtain decreasing function in agreement with experiments [47,69]. Equation (28) corresponds to the direct relaxation into the phonon reservoir. At high temperatures the Raman process can be effective. Its rate is proportional to T^7 (and, correspondingly, $W \sim T^{\check{S}\,7}$). Indeed, the intensity of the "exciton-magnon" lines in $MnCO_3$ decreases with the temperature rising faster than according to (28) [47]. We saw above that at $T = 0$ K the probability W_e can be substantially different function of J, depending on type of the exchange interaction, on the value of S-L interaction (mainly in the excited state) and on the peculiarity of the phonon spectrum of the substance under consideration. As mentioned above, coefficient k_e of the bonding between electron and spin excitations of the pair is an increasing function of the exchange and S-L interactions. The latter depends on the type of the excited state and on the crystal field. Thus, the intensity of the electron-spin ("exciton-magnon") lines (and even their existence at all) is a complicated and practically not predictable function of the magnetic and crystal structure and of the electronic excited state of the atom: the vary thing observed in experiments.

Nature of the *d-d* absorption line widths is the last problem that it is worth discussing. Considered excitations are not strictly local, but quasi local ones. They are localized not in one elementary cell of a crystal and therefore create not a single level but a band of levels, giving one of contributions into the line width. The delocalization transforms a monochromatic, purely local excitation into an energy band of the quasi-local excitations. The delocalization of the vibronic excitations increases with the increase of the electron-lattice interaction. The latter can be estimated with the help of the Tanabe-Sugano diagrams [70]: the stronger the level energy depends on the crystal field – the stronger is the electron-lattice interaction. Thus, A and B "exciton-magnon-phonon" bands should be wider than the "exciton-magnon-phonon" C-band: the very thing observed in experiments, the present experiment including (see Fig. 2). The specific band width depends also on the value of the electron-vibration interaction and on the number and energy of active odd vibrations. So, the vibronic lines, being very wide for the bands A and B, overlap and create additional effective broadening of these bands. The same mechanisms of the broadening are, evidently, valid for the one ion absorption as well. That is why the shape of the absorption bands of the one ion and of the collective exchange-vibronic transitions is similar. The second source of the line widths is the relaxation of the excitations. The relaxation rate in a first approximation is the sum of the relaxation rates of all excitations involved in the bound state. Therefore, the width of the "exciton-magnon" lines should be significantly smaller than the width of the "exciton-magnon-phonon" lines. This is indeed observed: e.g., narrow "exciton-magnon" lines against the background of the wide "exciton-magnon-phonon" band of $^6A_1 \rightarrow {}^4T_1$ transition in $FeBO_3$ [69]. The former of mentioned above broadening mechanisms should almost not depend on temperature, while the latter one should strongly depend on temperature that permits us to identify the nature of absorption bands widths. In particular, the width of the A- and B-bands almost does not change with the temperature (Fig. 2), but "exciton-magnon-phonon" lines, which C-band is composed from (see Figs. 2, 3 and also [48]), and all "exciton-magnon" lines (e.g., [47]) get narrow with the decreasing temperature, that indicate the prevailing broadening mechanism: the delocalization for A and B "exciton-magnon-phonon" bands; relaxation for C "exciton-magnon-phonon" lines and for all "exciton-magnon" lines.

3 Summary

Single crystals of $GdFe_{2.1}Ga_{0.9}(BO_3)_4$ and $GdFe_3(BO_3)_4$ compounds have been grown and their polarized optical absorption spectra and linear birefringence have been measured in the temperature range 85–293 K. Crystal structure of $GdFe_{2.1}Ga_{0.9}(BO_3)_4$ has been studied and its specific heat has been measured in the temperature range 2–300 K. The structure of $GdFe_{2.1}Ga_{0.9}(BO_3)_4$ coincided

with that of $GdFe_3(BO_3)_4$. A feature at $T = 16$ K was revealed on the specific heat temperature dependence of $GdFe_{2.1}Ga_{0.9}(BO_3)_4$, which corresponds to the magnetic phase transition. Structural phase transition in $GdFe_{2.1}Ga_{0.9}(BO_3)_4$ was not observed. As a result of substitution of 30% Fe to Ga the Neel temperature diminishes from 38 till 16 K, the strong absorption band edge shifts on 860 cm^{-1} (0.11 eV) to higher energy and the *d-d* transitions intensity decreases substantially larger than the Fe concentration does. The jump of the first temperature derivative of the strong absorption band edge position at 156 K both in $GdFe_3(BO_3)_4$ and $GdFe_{2.1}Ga_{0.9}(BO_3)_4$ testifies to the similar features in the temperature behavior of the lattice parameters and of the electron-phonon interaction in these crystals, that, nevertheless, is not realized in a structural phase transition in $GdFe_{2.1}Ga_{0.9}(BO_3)_4$ crystal. The strong absorption band edge in the region of 25 000 cm^{-1} (3.1 eV) is due to interatomic Fe−Fe *d-d* excitations (Mott-Hubbard transitions). The linear birefringence near the strong absorption band edge is also mainly conditioned by the same transitions. It has been found out that the energy of the strong absorption band edge correlates with the Neel temperature of compounds (it increases, when the Neel temperature decreases) since both, the Fe−Fe transitions and the exchange interaction, are conditioned by the overlapping of the Fe^{3+} molecular orbitals.

Properties of the doubly forbidden *d-d* transitions in the studied crystals and in other antiferromagnetic compounds are explained by the exchange-vibronic model of the pair absorption. This model makes possible to present the probability of the doubly forbidden *d-d* transitions as the product of probabilities of the vibronic and exchange stimulated absorption processes for the transitions forbidden only by parity and by spin selection rules respectively. Both of them have their own temperature dependences connected with the thermal population of vibrational or magnetic states, respectively. However these dependences do not describe experimentally observed temperature dependences of intensities of the doubly forbidden *d-d* transitions in antiferromagnets. Taking into account the relaxation of the exciton-magnon-phonon and exciton-magnon bound states, appeared as a result of a photon absorption by the pair of the exchange coupled ions, we have explained all variety of temperature dependences of the doubly forbidden *d-d* transitions intensities in antiferromagnets. The absorption band width depends on the relaxation and delocalization of the excitation. Taking into account these contributions, the nature of widths of different absorption bands has been explained. Parameter of bonding between the vibronic and the magnetic excitations is an increasing function of the product of parameters of the exchange and S-L interactions. As a consequence, existence of the exchange-vibronic absorption is connected not only with the exchange interaction, but also with the type of the excited state: if the excited state has orbital moment, then the exchange-vibronic absorption appears at a smaller exchange interaction. Intensity of the exchange-vibronic absorption is a complicated function of the exchange interaction, since the exchange interaction presents not only in the initial formula of the exchange-vibronic absorption, but it also influences the bonding strength and the relaxation rate of the exciton-magnon-phonon bound state.

The work was supported by the Russian Foundation for Basic Researches Grant 12-02-00026 and by Russian President Grant NSh-1044.2012.2.

References

1. W.A. Dollase, R.J. Reeder, Amer. Miner. **71**, 163 (1986)
2. X. Chen, Z. Luo, D. Jaque, J.J. Romero, J.G. Sole, Y. Huang, A. Jiang, C. Tu, J. Phys.: Condens. Matter **13**, 1171 (2001)
3. A.N. Vasiliev, E.A. Popova, Fiz. Niz. Temp. **32**, 968 (2006) [Low Temp. Phys. **32**, 735 (2006)]
4. A.K. Zvezdin, S.S. Krotov, A.M. Kadomtseva, G.P. Vorob'ev, Y.F. Popov, A.P. Pyatakov, L.N. Bezmaternykh, E.A. Popova, Pis'ma v ZhETF **81**, 335 (2005) [JETP Lett. **81**, 272 (2005)]
5. A.K. Zvezdin, G.P. Vorob'ev, A.M. Kadomtseva, Yu.F. Popov, A.P. Pyatakov, L.N. Bezmaternykh, A.V. Kuvardin, E.A. Popova, Pis'ma v ZhETF **83**, 600 (2006) [JETP Lett. **83**, 509 (2006)]
6. F. Yen, B. Lorenz, Y.Y. Sun,1 C.W. Chu, L.N. Bezmaternykh, A.N. Vasiliev, Phys. Rev. B **73**, 054435 (2006)
7. A.M. Kadomtseva, Yu.F. Popov, G.P. Vorob'ev, A.A. Muhin, V.Yu. Ivanov, A.M. Kuzmenko, L.N. Bezmaternykh, Pis'ma v ZhETF **87**, 45 (2008) [JETP Lett. **87**, 39 (2008)]
8. R.P. Chaudhury, F. Yen, B. Lorenz, Y.Y. Sun, L.N. Bezmaternykh, V.L. Temerov, C.W. Chu, Phys. Rev. B **80**, 104424 (2009)
9. G.A. Smolenskii, I.E. Chupis, Usp. Fiz. Nauk **137**, 415 (1982) [Sov. Phys. Usp. **25**, 475 (1982)]
10. W. Eerenstein, N.D. Mathur, J.F. Scott, Nature **442**, 759 (2006)
11. A.S. Moskvin, S.-L. Drechsler, Phys. Rev. B **78**, 024102 (2008)
12. A.D. Balaev, L.N. Bezmaternykh, I.A. Gudim, V.L. Temerov, S.G. Ovchinnikov, S.A. Kharlamova, J. Magn. Magn. Mater. **258-259**, 532 (2003)
13. A.I. Pankrats, G.A. Petrakovskii, L.N. Bezmaternykh, O.A. Bayukov, JETP **99**, 766 (2004)
14. S.A. Kharlamova, S.G. Ovchinnikov, A.D. Balaev, M.F. Tomas, I.S. Lyubutin, A.G. Gavriliyuk, JETP Lett. **101**, 1098 (2005)
15. O.A. Bayukov, A.M. Gavrilyuk, V.N. Zabluda, I.S. Lyubutin, S.G. Ovchinnikov, A.M. Potseluyko, M. Tomas, I.A. Trojan, S.A. Kharlamova, Physica B **359-361**, 1321 (2005)
16. L.N. Bezmaternykh, S.G. Ovchinnikov, A.D. Balaev, S.A. Kharlamova, V.L. Temerov, A.D. Vasil'ev, J. Magn. Magn. Mater. **272-276S**, E359 (2004)
17. S.A. Klimin, D. Fausti, A. Meetsma, L.N. Bezmaternikh, P.H.M. van Loosdrecht, T.T.M. Palsta, Acta Cryst. B **61**, 481 (2005)

18. R.Z. Levitin, E.A. Popova, R.M. Chtshebrov, A.N. Vasiliev, M.N. Popova, E.P. Chukalina, S.A. Klimin, P.H.M. van Loosdrecht, D. Fausti, L.N. Bezmaternykh, Pis'ma v ZhETF **79**, 531 (2004) [JETP Lett. **79**, 423 (2004)]
19. M.N. Popova, T.N Stanislavchuk, B.Z Malkin, L.N. Bezmaternykh, Phys. Rev. B **80**, 195101 (2009)
20. A.G. Gavrilyuk, S.A. Kharlamova, I.S. Lubutin, I.A. Troyan, S.G. Ovchinnikov, A.M. Potseluiko, M.I. Eremets, R. Boehler, JETP Lett. **80**, 426 (2004)
21. A.M. Kalashnikova, V.V. Pavlov, R.V. Pisarev, L.N. Bezmaternykh, M. Bayer, Th. Rasing, Pis'ma v Zhetf **80**, 339 (2004) [JETP Lett. **80**, 293 (2004)]
22. V.N. Zabluda, S.G. Ovchinnikov, A.M. Potseluiko, S.A. Kharlamova, Phys. Solid State **47**, 489 (2005)
23. A.M. Clogston, J. Appl. Phys. **31**, 198S (1960)
24. K.A. Wickersheim, R.A. Lefever, J. Chem. Phys. **36**, 844 (1962)
25. S.G. Ovchinnikov, V.N. Zabluda, Zh. Exp. Teor. Fiz. **125**, 150 (2004) [J. Exp. Theor. Phys. **98**, 135 (2004)]
26. N.N. Kovaleva, A.V. Boris, C. Bernhard, A. Kulakov, A. Pimenov, A.M. Balbashov, G. Khaliullin, B. Keimer, Phys. Rev. Lett. **93**, 147204 (2004)
27. J.L. Pascual, B. Savoini, R. González, Phys. Rev. B **70**, 045109 (2004)
28. S. Picozzi, K. Yamauchi, B. Sanyal, I.A. Sergienko, E. Dagotto, Phys. Rev. Lett. **99**, 227201 (2007)
29. A.S. Moskvin, R.V. Pisarev, Phys. Rev. B **77**, R060102 (2008)
30. A.S. Moskvin, A.A. Mahnev, L.V. Nomerovannaya, N.N. Loshkareva, A.M. Balbashov, Phys. Rev. B **82**, 035106 (2010)
31. R. Loudon, Adv. Phys. **17**, 243 (1968)
32. V.V. Eremenko, E.G. Petrov, Adv. Phys. **26**, 31 (1977)
33. V.V. Eremenko, N.F. Kharchenko, Yu.G. Litvinenko, V.M. Naumenko, *Magneto-Optics and Spectroscopy of Antiferromagnets* (Springer-Verlag, 1992)
34. *Magneto-Optics*, edited by S. Sugano, N. Kojima (Berlin, Springer, 2000)
35. B. Fromme, *d-d Excitations in Transition-Metal Oxides* (Berlin, Springer, 2001)
36. Y. Tanabe, T. Moriya, S. Sugano, Phys. Rev. Lett. **15**, 1023 (1965)
37. J. Ferguson, H.J. Guggenheim, Y. Tanabe, J. Phys. Soc. Jpn **21**, 692 (1966)
38. J. Ferguson, H.J. Guggenheim, Y. Tanabe, Phys. Rev. **161**, 207 (1967)
39. V.V. Druzhinin, R.V. Pisarev, G.A. Karamisheva, Fiz. Tverd. Tela **12**, 2239 (1970) [Sov. Phys. Solid State **12**, 1789 (1970)]
40. T. Fujiwara, W. Gebhardt, K. Petanides, Y. Tanabe, J. Phys. Soc. Jpn **33**, 39 (1972)
41. I. Harada, K. Motizuki, Solid State Commun. **11**, 171 (1972)
42. J. Ferguson, N.U. Güdel, E.R. Krausz, H.J. Guuenheim, Mol. Phys. **28**, 893 (1974)
43. N.S. Altshuler, M.V. Eremin, Fiz. Tverd. Tela **21**, 181 (1979)
44. C. Mathonière, O. Kahn, Inorg. Chem. **33**, 2103 (1994)
45. A.V. Malakhovskii, G.G. Vasiljev, Solid State Commun. **48**, 353 (1983)
46. A.V. Malakhovskii, Solid State Commun. **60**, 591 (1986)
47. A.V. Malakhovskii, V.S. Filimonov, E.A. Goncharov, Phys. Lett. A **138**, 412 (1989)
48. A.V. Malakhovskii, T.P. Morozova, Fiz. Tverd. Tela **48**, 266 (2006) [Physics of the Solid State **48**, 283 (2006)]
49. G.M. Sheldrick, *SHELXLS97 and SHELXL97* (University of Göttingen, Germany, 1997)
50. *Numerical Data and Functional Relationships in Science and Technology*, edited by O. Madelung, Landoldt-Börnstein (Springer-Verlag, Berlin, 1993), Group III, Vol. 27h
51. A.N. Vasiliev, E.A. Popova, I.A. Gudim, L.N. Bezmaternykh, Z. Hiroi, J. Magn. Magn. Mater. **300**, e382 (2006)
52. H.H. Tippins, Phys. Rev. B **1**, 126 (1970)
53. G.B. Scott, J.L. Page, Phys. Stat. Sol. B **79**, 203 (1977)
54. S. Hufner, Adv. Phys. **43**, 183 (1994)
55. J.I. Pankove, *Optical processes in semiconductors* (Prentice-Hall, Inc., Englewood Cliffs, New Jersey, 1971)
56. G.S. Krinchik, M. Kuchera, V.D. Gorbunova, V.S. Guschin, Fiz. Tverd. Tela **23**, 405 (1981)
57. A.V. Malakhovskii, I.S. Edelman, Phys. Stat. Sol. B **74**, K145 (1976)
58. G.B. Scott, D.E. Lacklison, J.L. Page, Phys. Rev. B **10**, 971 (1974)
59. K. Pastor, Phys. Stat. Sol. B **68**, K13 (1975)
60. A.V. Malakhovskii, G.G. Vasilev, Phys. Stat. Sol. B **118**, 337 (1983)
61. E.I. Rashba, Zh. Eksp. Teor. Fiz. **54**, 542 (1968) [Sov. Phys. JETP **27**, 292 (1968)]
62. M.A. Kozhushner, Zh. Eksp. Teor. Fiz. **60**, 220 (1971) [Sov. Phys. JETP **33**, 121 (1971)]
63. Yu.B. Gaididei, V.M. Loktev, Phys. Stat. Sol. B **63**, 709 (1974)
64. A. Abragam, B. Bleaney, *Electron paramagnetic resonance of transition ions* (Clarendon Press, Oxford, 1970)
65. D.I. Blohintsev, *Fundamentals of quantum mechanics* (Moscow, Nauka, 1976) (in Russian)
66. J.C. Gill, Proc. Phys. Soc. **79**, 58 (1962)
67. E.K. Henner, I.G. Shaposhnikov, Jh. Exp. Theor. Fiz. **82**, 211 (1982)
68. L.L. Lohr, D.S. McClure, J. Chem. Phys. **49**, 3516 (1968)
69. V.N. Zabluda, A.V. Malakhovskii, I.S. Edelman, Phys. Stat. Sol. B **125**, 751 (1984)
70. Y. Tanabe, S. Sugano, J. Phys. Soc. Jpn **9**, 753 (1954)